Higgs bosons from vector-boson fusion in e^+e^-, ep, and pp collisions

Duane A. Dicus and Scott S. D. Willenbrock
Center for Particle Theory and Theory Group, University of Texas, Austin, Texas 78712
(Received 3 June 1985)

We calculate the production of Higgs bosons via W- and Z-boson fusion in e^+e^-, ep, and pp collisions. Vector-boson fusion is the dominant contribution to Higgs-boson production in e^+e^- and pp collisions for heavy Higgs bosons and in ep collisions for all Higgs-boson masses. We determine the maximum Higgs-boson mass which is accessible in each type of collision.

I. INTRODUCTION

The Higgs boson remains as elusive today as when it was predicted over fifteen years ago.[1] This neutral, spinless particle is the remnant of the scalar field which is responsible for the spontaneous breakdown of $SU(2)\times U(1)$ symmetry and the generation of the masses of all the particles in the standard electroweak model. Although support for the electroweak theory has been mounting steadily, there is no direct experimental evidence for the Higgs boson. The detection of this particle is one of our greatest experimental challenges.

The elusiveness of the Higgs boson lies in the curious nature of its interactions with other particles. Unlike gauge bosons, which couple with universal strength to all particles with the same quantum numbers regardless of their mass, the Higgs boson couples more strongly to heavy particles. Hence any production mechanism for the Higgs boson must necessarily contain heavy particles, either real or virtual. This in turn requires very-high-energy accelerators which can produce these heavy particles at a sizable rate. Furthermore, once the Higgs boson is produced it will tend to decay into the heaviest pair of particles that is kinematically allowed since it couples most strongly to these particles. These decay products will then decay themselves, leading to final states containing several particles. Thus the Higgs boson is not only difficult to produce, it is also difficult to detect.

Although the couplings of the Higgs boson to other particles are prescribed by the standard model, its mass is not, which further complicates the search. Since different colliders will be able to explore different mass ranges, we should consider a variety of particle collisions. Typically there are several processes which contribute to Higgs-boson production at a given collider. We have chosen to concentrate on vector-boson fusion since it is this process which allows us to produce the heaviest Higgs boson for a given collider energy. Thus the goal of our work is to determine the maximum Higgs-boson mass which will be accessible to future colliders.

In the following sections we will study separately the production of Higgs bosons via vector-boson fusion in e^+e^-, ep, and pp collisions. In the e^+e^- and pp cases our work is an extension or modification of the work of other authors, and we shall indicate this in the appropriate place.

Finally, a few words about our calculations. All cross sections involving hadrons are calculated with the parton model, using set 2 ($\Lambda=290$ MeV) of the distribution functions of Eichten, Hinchliffe, Lane, and Quigg (EHLQ).[2] We have used the gauge-boson masses $M_W=82$ GeV and $M_Z=93$ GeV throughout, as well as $\sin^2\theta_W=0.22$. The top-quark mass is taken[3] to be $m_t=40$ GeV. Expressions for the cross sections are gathered in an appendix in general forms which may be applied to e^+e^-, ep, and pp collisions.

II. e^+e^- COLLISIONS

Electron-positron collisions offer the cleanest laboratory for the study of the Higgs boson. This is of particular importance since the decay of the Higgs boson leads to multiparticle final states. The drawback is that e^+e^- colliders are somewhat restricted in energy, and thus will be useful to search for only relatively light Higgs bosons.

The goal of this section is to estimate the maximum Higgs-boson mass which may be reached by a given e^+e^- collider. This problem was first studied by Jones and Petcov[4] several years ago. Although we agree with their results qualitatively, we believe that they included interference effects with the wrong sign, and we have taken the opportunity to correct this. Also, we have taken into account the top-quark mass, which they had neglected. We have chosen to study center-of-mass energies $\sqrt{s}=140$ and 180 GeV with the hope that these will be attained by CERN LEP II in the not too distant future. The reach of a much higher energy e^+e^- collider ($\sqrt{s}=1$–2 TeV) has been studied in Ref. 5.

If the Higgs boson is sufficiently light, we may take advantage of the large cross section for Z production and hunt for the Higgs boson in the decay products[6–8] of the Z. The same technique may similarly be used at the t-quarkonium resonance.[9] Here we are interested in considering a Higgs boson which is too heavy for either of these processes to be feasible.

The diagrams which contribute to Higgs-boson production are shown in Fig. 1. There is also a contribution from Higgs bremsstrahlung off a produced fermion pair.[8,10] Since the Higgs boson coupling to fermions is proportional to their mass, this process is only important for the top quark. This would require sufficient energy to produce both a Higgs boson and a pair of top quarks.

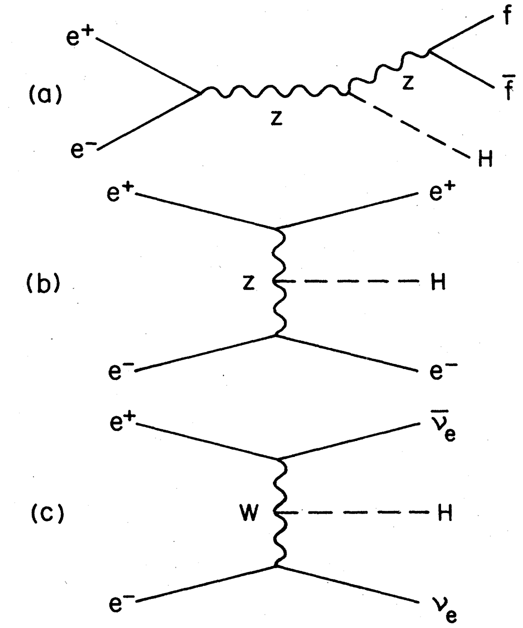

FIG. 1. Feynman diagrams contributing to Higgs-boson production in e^+e^- collisions: (a) bremsstrahlung from a Z boson, (b) Z-boson fusion, and (c) W-boson fusion.

This process is thus not pertinent to determining the reach of a given collider, so we will ignore it.

The cross sections for Higgs-boson production in e^+e^- collisions are shown in Figs. 2 and 3. The curves are labeled by the final states produced. The final states $H\mu^+\mu^-$ and $Hq\bar{q}$ receive contributions from diagram 1(a) only. The process $H\tau^+\tau^-$ is the same as $H\mu^+\mu^-$. The $Hq\bar{q}$ curve is the sum of contributions from all flavors of quarks. We have included the effect of the quark mass, which is non-negligible only for the top quark ($m_t=40$

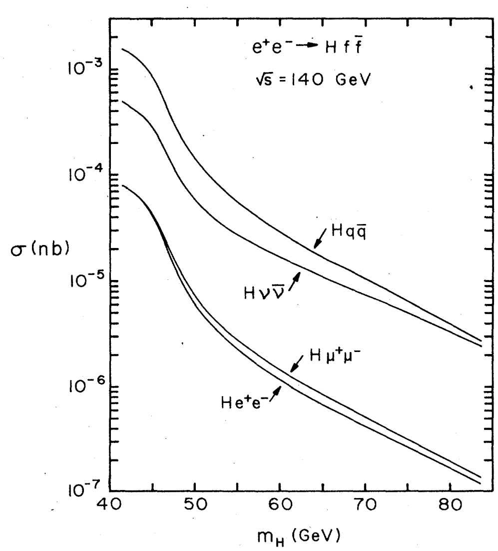

FIG. 2. Cross section for Higgs-boson production in e^+e^- collisions at center-of-mass energy 140 GeV vs the mass of the Higgs boson. The curves are labeled by the particles in the final state.

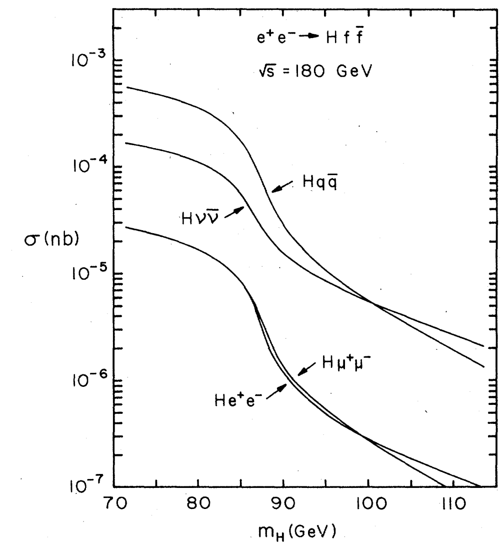

FIG. 3. Same as Fig. 2, but at center-of-mass energy 180 GeV.

GeV). The final state He^+e^- receives contributions from diagrams 1(a) and 1(b). The diagrams interfere destructively, resulting in cross sections below those for $H\mu^+\mu^-$. The $H\nu\bar{\nu}$ curve is the sum over all neutrino species, which we have assumed to be three in number. The process $H\nu_e\bar{\nu}_e$ receives contributions from diagrams 1(a) and 1(c), and the interference is constructive. The other two neutrino species are produced via diagram 1(a) only. Formulas for the cross sections may be found in the Appendix.

The curves in Figs. 2 and 3 fall dramatically at a Higgs-boson mass of about $m_H=\sqrt{s}-M_Z$. This is the point at which there is not enough energy for the second Z in diagram 1(a) to be on shell.[11] For masses above this point the vector-boson fusion process in diagrams 1(b) and 1(c) is competitive with the s-channel diagram 1(a), and becomes relatively more important at larger center-of-mass energies $\sqrt{s}$ since the cross section due to diagram 1(a) decreases roughly like $s/(s-M_Z{}^2)^2$.

To assess the reach in Higgs-boson mass of an e^+e^- collider we will assume a luminosity of 10^{32} cm^{-2} s^{-1} and require a minimum rate of one event per week; this corresponds to a minimum cross section of 2×10^{-5} nb. Since the Higgs boson does not decay into clean final states, the best method of detection is by missing-mass techniques. This entails measuring the energy and momentum of the leptons recoiling against the Higgs boson in either He^+e^- or $H\mu^+\mu^-$ and using this information to reconstruct the Higgs-boson mass.[6] Unfortunately, these cross sections are quite low, so this method is limited to Higgs-boson masses below 48 GeV at $\sqrt{s}=140$ GeV and 84 GeV at $\sqrt{s}=180$ GeV.

The production of Higgs bosons in association with neutrinos allows us to explore somewhat larger masses. Since the neutrinos will escape undetected, one must observe the decay products of the Higgs boson. A Higgs boson in the mass range we are considering will decay predominantly into $b\bar{b}$, producing a pair of jets. One must therefore look for the Higgs boson in the invariant-mass spectrum of jet pairs which are accompanied by missing energy. There is also the possibility that vertex detectors could be used to signal the presence of heavy quarks, which would greatly reduce the background from light-quark jet pairs.[8] The cross section for $H\nu\bar{\nu}$ is large enough to study Higgs bosons of masses up to 58 GeV at $\sqrt{s}=140$ GeV and 88 GeV at $\sqrt{s}=180$ GeV.

The reach of an e^+e^- collider may be extended even further if one observes the Higgs boson produced in association with a pair of quarks. The final state then contains four jets, two of which have a combined invariant mass equal to the Higgs-boson mass. Vertex detectors would again be useful for reducing the background.[8] Observing the Higgs boson in this mode of production allows one to study masses up to 64 GeV at $\sqrt{s}=140$ GeV and 92 GeV at $\sqrt{s}=180$ GeV.

III. *ep* COLLISIONS

In general, electron-proton collisions do not offer any distinct advantages over e^+e^- and *pp* collisions for the production of heavy particles. In a sense they combine the worst aspects of e^+e^- and *pp* collisions: the relatively low center-of-mass energies of e^+e^- collisions and the extra complexity of colliding a hadron beam. This is further complicated by the mismatch of electron and proton beam energies, which results in highly skewed kinematics. Nevertheless, a study of the potential use of *ep* collisions to produce Higgs bosons is warranted by the importance of this particle to our understanding of the electroweak interaction.

The first *ep* collider, the Hadron-Electron Ring Accelerator (HERA), is now under construction at DESY in Hamburg. It will produce collisions of total center-of-mass energy $\sqrt{s}=314$ GeV by colliding 30-GeV electrons with 820-GeV protons. Beyond this, there exists the possibility of *ep* collisions using the proton beam from the Superconducting Super Collider (SSC) in the United States or the Large Hadron Collider (LHC) at CERN. Assuming these beams will have energies of order 10 TeV, it will be possible to produce *ep* collisions of total energy above 1 TeV.

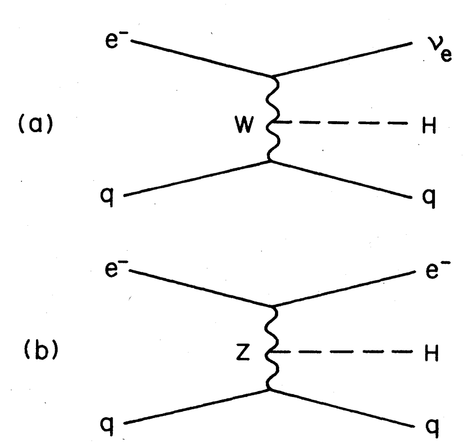

FIG. 4. Feynman diagrams contributing to Higgs-boson production in *ep* collisions: (a) *W*-boson fusion and (b) *Z*-boson fusion.

The most efficient means of producing the Higgs boson in *ep* collisions is via vector-boson fusion, as shown in Fig. 4. Because the coupling of the Z to fermions is somewhat weaker than that of the W, the charged-current process of Fig. 4(a) dominates. This is somewhat tempered by the fact that the negatively charged W may only interact with the positively charged quarks while the Z interacts with all quarks. The result is that Z-boson fusion contributes about 10% as much as W-boson fusion to the production of the Higgs boson. The Higgs boson may also be produced from photon fusion via virtual-fermion and W-boson loops. We have estimated the cross sections for this process to be small, less than 10^{-6} nb for the energies we are considering, and we will therefore neglect it.[12,13]

The total cross sections for Higgs-boson production from W- and Z-boson fusion are shown in Fig. 5. The curve $\sqrt{s}=314$ GeV corresponds to the HERA energy. The curves $\sqrt{s}=1$, 2, and 4 TeV correspond to electron energies of 25, 100, and 400 GeV for a proton beam of 10 TeV and to electron energies of 12.5, 50, and 200 GeV for a proton beam of 20 TeV. Formulas for the cross sections may be found in the Appendix.

To estimate the reach in Higgs-boson mass of these colliders, we will require a minimum cross section of 2×10^{-5} nb. Figure 5 then shows that the maximum accessible Higgs-boson mass is 20 GeV at the HERA energy, and 200, 450, and 900 GeV at center-of-mass energies of 1, 2, and 4 TeV, respectively.

A Higgs boson of mass less than twice the top-quark mass will decay overwhelmingly into a pair of bottom quarks. If the Higgs-boson mass lies between $2m_t$ and $2M_W$ it will decay predominantly into a pair of top quarks. In both cases there is a severe background from quark pair production via photon-gluon fusion (Fig. 6). The expression for the cross section is given by Eq. (2.4) in Ref. 12. Let us assume optimistically that bottom- and

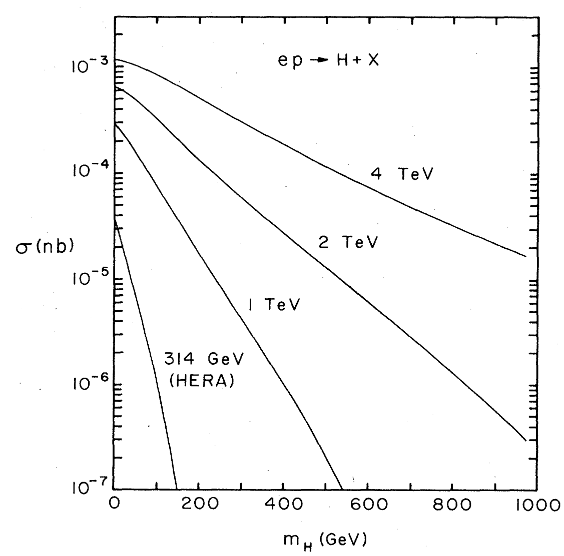

FIG. 5. Cross section for Higgs-boson production in *ep* collisions vs the mass of the Higgs boson. The curves are labeled by the center-of-mass energy of the collision.

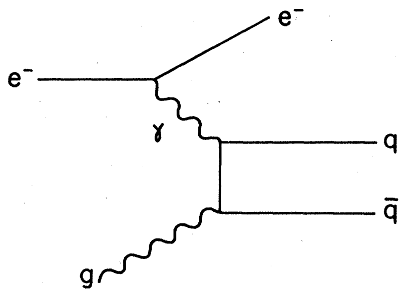

FIG. 6. Feynman diagram for quark pair production via photon-gluon fusion in *ep* collisions.

top-quark jets could somehow be identified, perhaps with the help of vertex detectors. In Fig. 7 we show the invariant-mass distribution of bottom-quark pairs and top-quark pairs at the various energies we are studying. Assuming an invariant-mass resolution of $\Delta M = 0.1 m_H$ yields a cross section $(d\sigma/dM)\Delta M$ for the background which dwarfs the signal from Higgs-boson production. We must therefore conclude that *ep* colliders will not be effective in detecting Higgs bosons less massive than $2M_W$. The same difficulty is well known to plague *pp* colliders.[14,15]

If the Higgs boson weighs more than $2M_W$ it will decay predominantly to a W-boson pair, and above $2M_Z$ it will decay to both W and Z pairs, in the ratio 2:1. These gauge bosons must then be reconstructed from their decay products. We do not anticipate any serious problems with the background from continuum W- and Z-pair production; however, the cross sections are not very large, so we must be able to identify W's and Z's very efficiently.

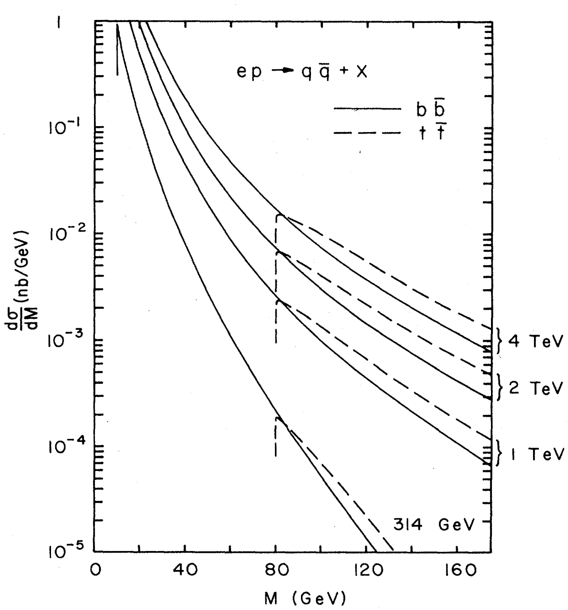

FIG. 7. Invariant-mass distribution $d\sigma/dM$ for quark pairs of invariant mass M produced in *ep* collisions. The solid lines are for bottom-quark pairs, the dashed lines for top-quark pairs. The curves are labeled by the center-of-mass energy of the collisions.

IV. *pp* COLLISIONS

Proton-proton collisions provide us with the opportunity to study very heavy Higgs bosons. There is hope that the SSC will attain center-of-mass energy $\sqrt{s} = 40$ TeV and the LHC $\sqrt{s} = 10$–20 TeV. One of the strongest motivations for building these machines is to search for the Higgs boson.

The principle production mechanism for Higgs bosons of mass less than a few hundred GeV is via gluon fusion[15] as shown in Fig. 8. The gluons couple to the Higgs boson via a virtual quark loop, which has the curious property that only heavy quarks contribute to the coupling. Roughly speaking, the process receives contributions from all quarks of mass $m_Q \gtrsim 0.2 m_H$. Since we are interested in heavy Higgs bosons, only the top quark contributes non-negligibly.

If we consider Higgs-boson masses greater than $5m_t$, even the top quark is too light to contribute sizably to the ggH interaction. The cross section for Higgs-boson production via gluon fusion then begins to decrease rapidly with increasing Higgs-boson mass. One should keep in mind that this conclusion is altered if there exist additional generations of quarks.

Cahn and Dawson[16] have shown that a very heavy Higgs boson is produced more efficiently by vector-boson fusion than by gluon fusion. The same calculation was later performed by EHLQ.[2] We have extended the calculations of these groups in two respects. First, we have used exact formulas for the cross sections, as given in the Appendix, rather than approximate ones. Second, we have included not only the s-, t-, and u-channel diagrams shown in Fig. 9, but also the interference between the diagrams in the first column with their counterparts in the second. We have found that the s-channel and interference contributions are negligible, as we will discuss shortly. Consequently we are in close agreement with the results of the above authors, which indicates that their approximation is indeed a very good one.[17]

In Fig. 10 we show the cross sections for Higgs-boson production via gluon fusion and vector-boson fusion in *pp* collisions. We see that vector-boson fusion begins to overtake gluon fusion for Higgs-boson masses above 350 GeV. The Higgs-boson signal and the background to that signal are discussed in detail by EHLQ (Ref. 2) and we refer the interested reader to their work. They conclude that a 40-

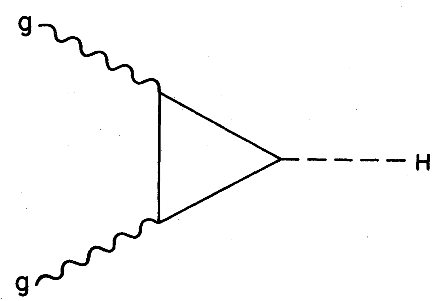

FIG. 8. Feynman diagram for Higgs-boson production via gluon fusion in *pp* collisions. The particle in the loop is a virtual quark.

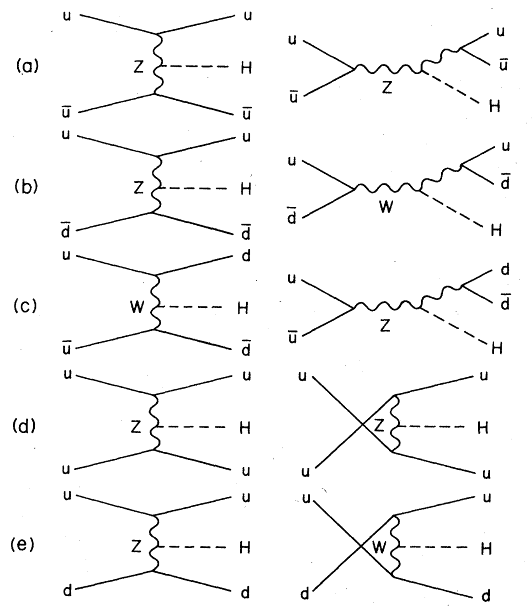

FIG. 9. Feynman diagrams contributing to Higgs-boson production in pp collisions: (a)—(c) parton collisions involving both an s- and t- channel diagram and (d) and (e) parton collisions involving both a t- and u-channel diagram.

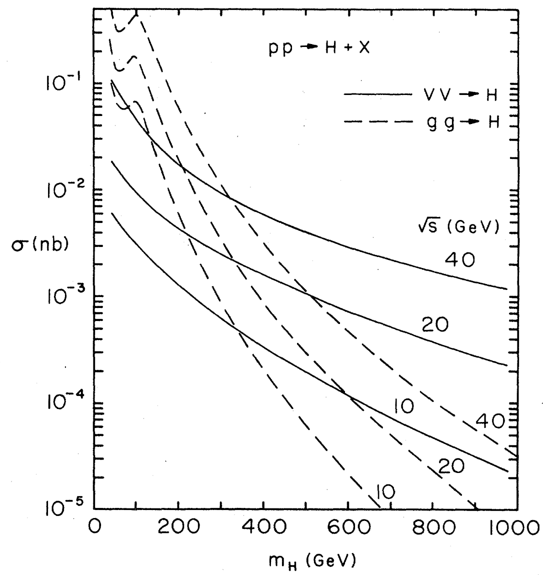

FIG. 10. Cross section for Higgs-boson production in pp collisions vs the mass of the Higgs boson. The solid lines are from W- and Z-boson fusion, the dashed lines from gluon fusion. The curves are labeled by the center-of-mass energy of the collision.

TeV pp collider with integrated luminosity 10^{40} cm^{-2} may be able to detect Higgs bosons as heavy as 1 TeV.

We conclude this section with a discussion of the calculation. In Fig. 9 we show all the diagrams which contribute to heavy-Higgs-boson production in pp collisions. The appropriate diagrams depend on the parton process under consideration. In particular, $u\bar{u}$ and $d\bar{d}$ collisions proceed via both 9(a) and 9(c); $u\bar{d}$ and $d\bar{u}$ via 9(b); uu, dd, $\bar{u}\bar{u}$, and $\bar{d}\bar{d}$ via 9(d); and ud and $\bar{u}\bar{d}$ via 9(e). All s-channel processes must be multiplied by $\frac{1}{3}$ since only quarks of the same color may interact. The same is true of all interference terms. The same diagrams occur for the second and third generation quarks as well. If the colliding partons are not members of the same $SU(2)_L$ doublet then they interact solely via t-channel exchange (ignoring Cabibbo mixing).

As Cahn and Dawson[15] have shown, the contribution to heavy-Higgs-boson production from the s-channel diagrams in Fig. 9 is small. This is a result of the high subprocess energies $(\hat{s})^{1/2}$ required and the fact that the cross section decreases roughly like $\hat{s}/(\hat{s}-M_Z{}^2)^2$. The interference between the s and t channel diagrams in Figs. 9(a)—9(c) is even smaller still since not only does it decrease like $1/(\hat{s}-M_Z{}^2)$ but it also vanishes when the second Z is on shell. What is perhaps not so obvious is that the interference between the t- and u-channel diagrams in Figs. 9(d) and 9(e) is also negligibly small. We may understand this qualitatively in the following way. Because of the vector-boson propagators, the integrand of the phase-space integral includes the factors

$$\frac{1}{(2p_1\cdot p_1'+M^2)}\,\frac{1}{(2p_2\cdot p_2'+M^2)}\,\frac{1}{(2p_1\cdot p_2'+M^2)}\,\frac{1}{(2p_2\cdot p_1'+M^2)}\;,$$

where p_1,p_2 are the incoming and p_1',p_2' are the outgoing fermion momenta, and M is the appropriate gauge-boson mass. Each factor is largest when the momentum dependence in the denominator is small compared to M^2. However, there is no region in phase space where more than two of these dot products are small. For example, the first two factors are largest if p_1' is collinear with p_1 and p_2' is collinear with p_2 so that $p_1\cdot p_1'=p_2\cdot p_2'=0$, but this is exactly the configuration where the last two factors are the smallest. Contrast this with the integrand of the square of the t-channel diagram, which contains

$$\left[\frac{1}{2p_1\cdot p_1'+M^2}\right]^2\left[\frac{1}{2p_2\cdot p_2'+M^2}\right]^2$$

and hence is the product of four large factors in the region of phase space considered above. The result is that the interference term is negligibly small.

V. CONCLUSIONS

In this paper we have explored the reach in Higgs-boson mass of future e^+e^-, ep, and pp colliders. In all cases the maximum mass is produced by vector-boson fusion. We have found that an e^+e^- collider of center-of-mass energy 140 (180) GeV will be able to hunt for Higgs bosons of masses up to 50—60 (80—90) GeV. Heavier Higgs bosons, up to 1 TeV in mass, will be best sought by pp collisions of energy on the order of tens of

TeV. Heavy Higgs bosons may also be found in *ep* collisions of center-of-mass-energy on the order of 1 TeV.

Note added in proof. After this paper was accepted for publication, several more papers on Higgs-boson production were brought to our attention. R. Bates and J. N. Ng [Phys. Rev. D **32**, 51 (1985)] have studied Higgs-boson production in polarized e^+e^- collisions at CERN LEP I and II energies. In another paper [TRIUMF Report No. TRI-PP-57 (unpublished)] they consider Higgs-boson production in *ep* collisions via both photon fusion and *Z*-boson fusion. Z. Hioki, S. Midorikawa, and H. Nishiura [Prog. Theor. Phys. **69**, 1484 (1983)] have also considered Higgs-boson production in *ep*, collisions, as well as νp collisions, in each case concentrating on interactions which result in a charged lepton in the final state. Finally, another paper on Higgs-boson production in $p\bar{p}$ collisions has recently appeared [R. N. Cahn, Nucl. Phys. **B255**, 341 (1985)]. We are in agreement with the results of these authors where their work overlaps ours.

ACKNOWLEDGMENTS

We would like to thank C. Burgess, S. Nandi, and J. Polchinski for interesting discussions. The work of D.A.D. was supported in part by the U.S. Department of Energy; the work of S.S.D.W. was supported by the National Science Foundation under Grant No. PHY83-04629 and in part by the Robert A. Welch Foundation.

APPENDIX

We present formulas for the spin-averaged cross sections which contribute to $ff \to Hff$, where f denotes the appropriate fermions. The couplings depend on both the fermions and the gauge bosons involved in the process, and we list them in Table I. With each expression we indicate the diagrams in the text to which it corresponds.

The expressions given are valid in any frame moving parallel to the beam axis, although the limits of integration are frame dependent. We give the integration limits for the center-of-mass frame, which is the most convenient in practice. Below we define some of the symbols used:

$s=(p_1+p_2)^2$ = square of the center-of-mass energy,

E_H = energy of the Higgs boson,

TABLE I. The couplings used in the Appendix on the cross sections for $ff \to Hff$, where f denotes the appropriate fermions. g_H is the coupling of the Higgs boson to the W and Z vector bosons, and g_L, g_R are the gauge couplings of fermions of charge Q and weak isospin $T_{3L}(=\pm\frac{1}{2})$.

	W	Z
g_H	M_W	$\dfrac{M_z}{\cos\theta_W}$
g_L	$\dfrac{1}{2\sqrt{2}}$	$\dfrac{1}{2\cos\theta_W}(T_{3L}-Q\sin^2\theta_W)$
g_R	0	$-\dfrac{1}{2\cos\theta_W}Q\sin^2\theta_W$

z_H = cosine of the angle between the Higgs-boson momentum vector and the beam axis,

M = mass of the appropriate vector boson,

Γ = width of the appropriate vector boson,

$|\mathbf{p}_H| = (E_H{}^2 - M_H{}^2)^{1/2}$ = magnitude of the Higgs-boson momentum,

$y = s + m_H{}^2 - 2(p_1+p_2)\cdot p_H$ = invariant mass squared of the final fermions.

The limits of integration of E_H are

$$m_H \le E_H \le \frac{1}{2\sqrt{s}}(s+m_H{}^2) ,$$

except in the s-channel cross section via Z exchange where the upper limit is $(1/2\sqrt{s})(s+m_H{}^2-4m^2)$, where m is the mass of the produced fermion.

A. s channel

This corresponds to Fig. 1(a) and the second diagram in Figs. 9(a)—9(c). In the case where the vector boson is a Z we have kept terms proportional to the mass squared of the produced fermion, since these terms are important in our analysis of Higgs-boson production at an e^+e^- collider. In the case of W exchange we have ignored the masses of the produced fermions, since this process only occurs in pp collisions and is negligibly small at the energies we are considering. Thus the formula below is correct for W exchange only in the $m=0$ limit:

$$\sigma = \frac{4}{3}\frac{\alpha^3}{\sin^6\theta_W}(g_L{}^2+g_R{}^2)g_H{}^2\frac{s}{(s-M^2)^2}\int dE_H\,|\mathbf{p}_H|\left[1-\frac{4m^2}{y}\right]^{1/2}\frac{1}{(y-M^2)^2+M^2\Gamma^2}$$
$$\times\left\{(g_V'^2+g_A'^2)\left[1+\frac{2}{3}\frac{m_H{}^2}{s}-2\frac{E_H}{\sqrt{s}}+\frac{1}{3}\frac{E_H{}^2}{s}\right.\right.$$
$$\left.\left.-\frac{m^2}{y}\left[1+\frac{5}{3}\frac{m_H{}^2}{s}-2\frac{E_H}{\sqrt{s}}-\frac{2}{3}\frac{E_H{}^2}{s}\right]\right]\right.$$
$$\left.+3\frac{m^2}{s}\left\{g_V'^2-g_A'^2\left[1+\frac{4}{3}\frac{|\mathbf{p}_H|^2}{M^2}\left[1+\frac{y}{2M^2}\right]\right]\right\}\right\} ,$$

where m is the mass of the final fermion (Z exchange only), $g_V'=g_L'+g_R'$, and $g_A'=g_L'-g_R'$, the primes referring to the final fermions. A factor of 3 should be included if the final fermions are quarks, and a factor of $\frac{1}{3}$ if the initial fermions are quarks.

B. t and u channel

This corresponds to Figs. 1(b) and 1(c), Figs. 4(a) and 4(b), and the first diagram in Figs. 9(a)—9(e) as well as the second diagram in Figs. 9(d) and 9(e). The formula given below is appropriate for a particle-particle or antiparticle-antiparticle collision; in the case of a particle-antiparticle collision, one should interchange the coefficients C_1 and C_2:

$$\sigma = 16\frac{\alpha^3}{\sin^6\theta_W}\frac{g_H{}^2}{s} \times \int dE_H\,|\mathbf{p}_H|\int_{-1}^{1}dz_H\int_0^1 du\left[C_1 u(1-u)sy\frac{3a^2+b^2}{(a^2-b^2)^3}+C_2\left[\alpha_1\alpha_2 u(1-u)\frac{3a^2+b^2}{(a^2-b^2)^3} -[\alpha_1(1-u)+\alpha_2 u]\frac{a}{(a^2-b^2)^2}+\frac{1}{2}\frac{1}{a^2+b^2}\right]\right],$$

where

$$C_1=g_{1L}{}^2g_{2L}{}^2+g_{1R}{}^2g_{2R}{}^2,\quad C_2=g_{1L}{}^2g_{2R}{}^2+g_{1R}{}^2g_{2L}{}^2\,,$$

and

$$\alpha_1=s-2p_1\cdot p_H+M^2,\quad \alpha_2=s-2p_2\cdot p_H+M^2,\quad a=\tfrac{1}{2}s-p_1\cdot p_H(1-u)-p_2\cdot p_H u+M^2\,,$$

$$b^2=\tfrac{1}{4}(s-2p_1\cdot p_H)^2(1-u)+\tfrac{1}{4}(s-2p_2\cdot p_H)^2u-u(1-u)\{[p_H\cdot(p_1+p_2)]^2-sm_H{}^2\}\,.$$

C. Interference between s and t channels

This corresponds to the interference of the diagrams in Figs. 1(a) and 1(b), Figs. 1(a) and 1(c), and the first and second diagrams in Figs. 9(a)—9(c):

$$\sigma=2\frac{\alpha^3}{\sin^6\theta_W}C\frac{g_H^i g_H^j}{s}\frac{1}{s-M_i{}^2} \times\int dE_H\,|\mathbf{p}_H|\int_{-1}^{1}dz_H\int_0^1 du\frac{y-M_i{}^2}{(y-M_i{}^2)^2+M_i{}^2\Gamma_i{}^2} \times\left[1+\alpha_1\alpha_2\frac{1}{a^2-b^2}-\frac{\alpha_1}{\alpha_1-M_j{}^2}\ln\frac{\alpha_1}{M_j{}^2}-\frac{\alpha_2}{\alpha_2-M_j{}^2}\ln\frac{\alpha^2}{M_j{}^2}\right],$$

where

$$C=\begin{cases}8(g_L{}^4+g_R{}^4) & \text{for } Z \text{ in both channels,}\\ g_{1L}g_{2L} & \text{for } Z \text{ in one channel and } W \text{ in the other}\,.\end{cases}$$

The g's above are the couplings to the Z. The index i (j) refers to the gauge boson in the s (t) channel. α_1, α_2, a, and b^2 are as given above with M equal to the t-channel vector-boson mass. A factor of $\frac{1}{3}$ should be included if the fermions are quarks.

D. Interference between t and u channels

This corresponds to the interference of the first and second diagrams in Figs. 9(d) and 9(e):

$$\sigma=2\frac{\alpha^3}{\sin^6\theta_W}Cg_H^i g_H^j\int dE_H\,|\mathbf{p}_H|\,y\int_{-1}^{1}dz_H\frac{1}{D_1D_2}(I_{tu}^{+}+I_{ut}^{+}-I_{tt}^{-}-I_{uu}^{-})\,,$$

where C is given above. The index t (u) refers to the gauge boson in the t (u) channel. The denominators are

$$D_1=s-2p_1\cdot p_H+M_t{}^2+M_u{}^2,\quad D_2=s-2p_2\cdot p_H+M_t{}^2+M_u{}^2\,,$$

and the integrands are given by

$$I_{ij}^{\pm}=\frac{1}{(\Delta_\pm)^{1/2}}\ln\left|\frac{2a^{\pm}+b^{\pm}-(\Delta_\pm)^{1/2}}{2a^{\pm}+b^{\pm}+(\Delta_\pm)^{1/2}}\frac{b^{\pm}+(\Delta_\pm)^{1/2}}{b^{\pm}-(\Delta_\pm)^{1/2}}\right| ,$$

where

$$\Delta_\pm=b^{\pm 2}-4a^{\pm}c ,$$

$$a^{+}=-s^2+2sp_H\cdot(p_1+p_2)-sm_H{}^2+(M_i{}^2-M_j{}^2)^2-2(M_i{}^2-M_j{}^2)p_H\cdot(p_1+p_2) ,$$

$$a^{-}=4p_1\cdot p_H p_2\cdot p_H-sm_H{}^2+2(M_i{}^2+M_j{}^2)[s-p_H\cdot(p_1+p_2)]+(M_i{}^2+M_j{}^2)^2 ,$$

$$b^{+}=s^2-2sp_H\cdot(p_1+p_2)+sm_H{}^2-2M_j{}^2p_H\cdot(p_1-p_2)+(M_i{}^2-M_j{}^2)(s-2p_2\cdot p_H+2M_j{}^2) ,$$

$$b^{-}=-4p_1\cdot p_H p_2\cdot p_H+sm_H{}^2-2M_j{}^2[2s-2p_2\cdot p_H-p_H\cdot(p_1+p_2)]-2M_j{}^2(M_i{}^2+M_j{}^2) ,$$

$$c=M_j{}^2(s-2p_2\cdot p_H+M_j{}^2) .$$

A factor of $\frac{1}{3}$ should be included if the fermions are quarks, and a factor of $\frac{1}{2}$ if the final fermions are identical.

---

[1]S. Weinberg, Phys. Rev. Lett. **19**, 1264 (1967); A. Salam, in *Elementary Particle Theory: Relativistic Groups and Analyticity (Nobel Symposium No. 8)*, edited by N. Svartholm (Almqvist and Wiksell, Stockholm, 1968).

[2]E. Eichten, I. Hinchliffe, K. Lane, and C. Quigg, Rev. Mod. Phys. **56**, 579 (1984).

[3]UA1 Collaboration, G. Arnison *et al.*, Phys. Lett. **147B**, 493 (1984).

[4]D. R. T. Jones and S. T. Petcov, Phys. Lett. **84B**, 440 (1979).

[5]S. Dawson and J. L. Rosner, Phys. Lett. **148B**, 497 (1984).

[6]J. D. Bjorken, in *Weak Interactions at High Energy and the Production of New Particles*, proceedings of SLAC Summer Institute on Particle Physics, 1976, edited by M. Zipf (SLAC Report No. 198, 1977); E. Ma and J. Okada, Phys. Rev. D **20**, 1052 (1979).

[7]R. N. Cahn, M. S. Chanowitz, and N. Fleishon, Phys. Lett. **82B**, 113 (1979).

[8]V. Barger, F. Halzen, and W. Y. Keung, Phys. Lett. **110B**, 323 (1982).

[9]F. Wilczek, Phys. Rev. Lett. **39**, 1304 (1977).

[10]K. J. F. Gaemers and G. J. Gounaris, Phys. Lett. **77B**, 379 (1978).

[11]S. L. Glashow, D. V. Nanopoulos, and A. Yildiz, Phys. Rev. D **18**, 1724 (1978).

[12]J. A. Bagger and M. E. Peskin, Phys. Rev. D **31**, 2211 (1985).

[13]Our estimate for photon fusion agrees with a similar claim made in Ref. 12. However, our calculation does not agree with the estimate in Ref. 12 that W^+W^- fusion is also less than 10^{-6} nb.

[14]J. F. Gunion, P. Kalyniak, M. Soldate, and P. Galison, Phys. Rev. Lett. **54**, 1226 (1985).

[15]H. M. Georgi, S. L. Glashow, M. E. Machacek, and D. V. Nanopoulos, Phys. Rev. Lett. **40**, 692 (1978); K. J. F. Gaemers and F. Hoogeveen, Phys. Lett. **146B**, 347 (1984).

[16]R. N. Cahn and S. Dawson, Phys. Lett. **136B**, 196 (1984); **138B**, 464(E) (1984).

[17]We agree closely with the curves given in the errata of Ref. 16, not those in the original article.